Insights into the mechanism of electrode degradation and performance enhancing strategies for iron-ion batteries using X-ray absorption spectroscopy

Jitendra Kumar Yadav[1], Subhajit Nandy[2], Keun Hwa Chae[3], Jitendra Pal Singh[4], Ambesh Dixit[1,5*]

[1]Advanced Materials and Devices Laboratory, Department of Physics, Indian Institute of Technology Jodhpur, Jodhpur-342030, India

[2]Deutsches Elektronen-Synchrotron DESY, Notkestraβe 85, Hamburg 22607, Germany

[3]Advanced Analysis and Data Center, Korea Institute of Science and Technology (KIST), Seoul 02792, Republic of Korea

[4]Department of Sciences (Physics), Manav Rachna University , Faridabad, Haryana 121010, India

[5]Rishabh Centre for Research and Innovation in Clean Energy, Indian Institute of Technology Jodhpur, Jodhpur, Rajasthan-342030, India

*Corresponding author email: ambesh@iitj.ac.in

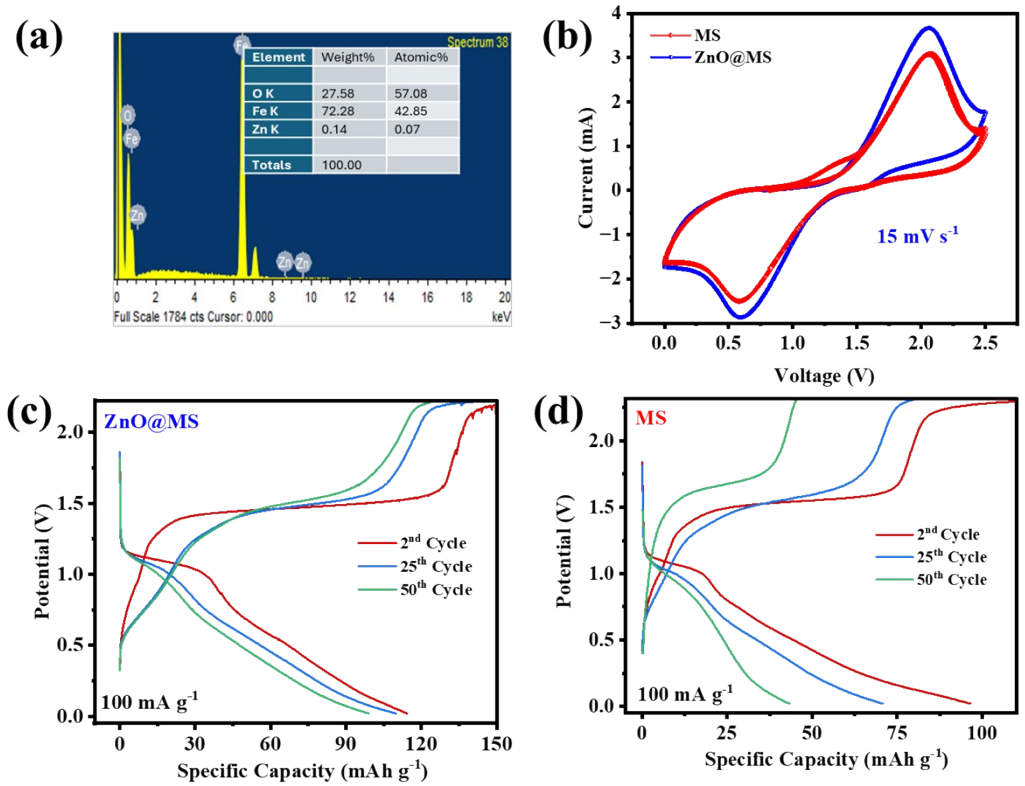

Figure S1: (a) EDAX spectrum corresponding to SEM of the ZnO@MS (b) the coin cell CV at 15 mV s^{-1} for the MS and ZnO@MS, Charge-discharge curve for various cycling stages at 100 mA g^{-1} (c) ZnO@MS based and(d) MS based coin cell

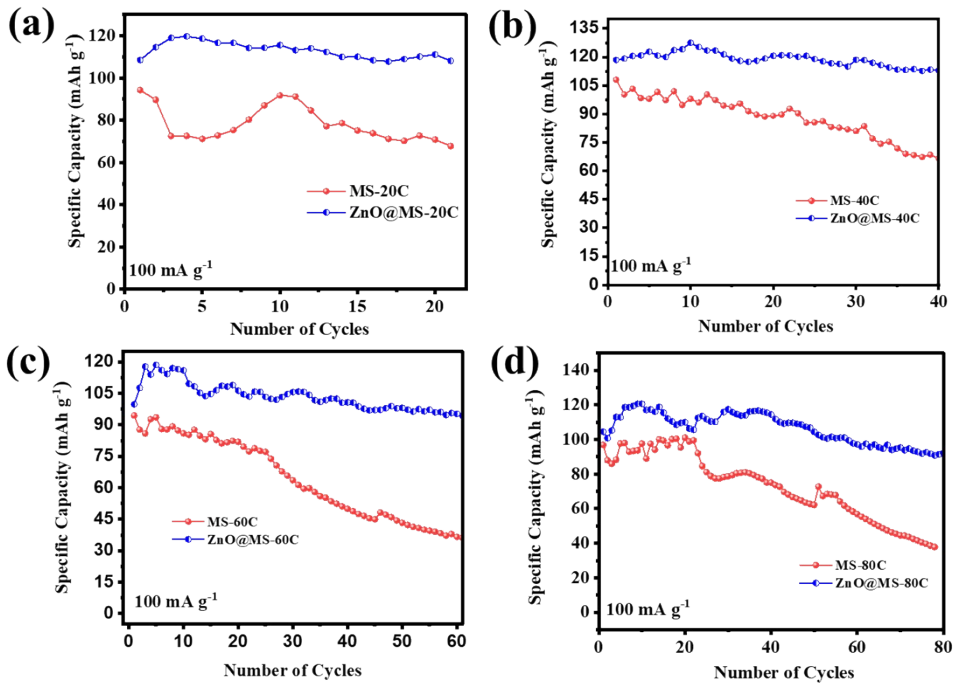

Figure S2: GCD analysis for specific capacity with the number of cycles for MS and ZnO@MS based coin cell for different cycling stages at 100 mA g^{-1} (a) 20 cycles, (b) 40 cycles, (c) 60 cycles, (d) 80 cycles

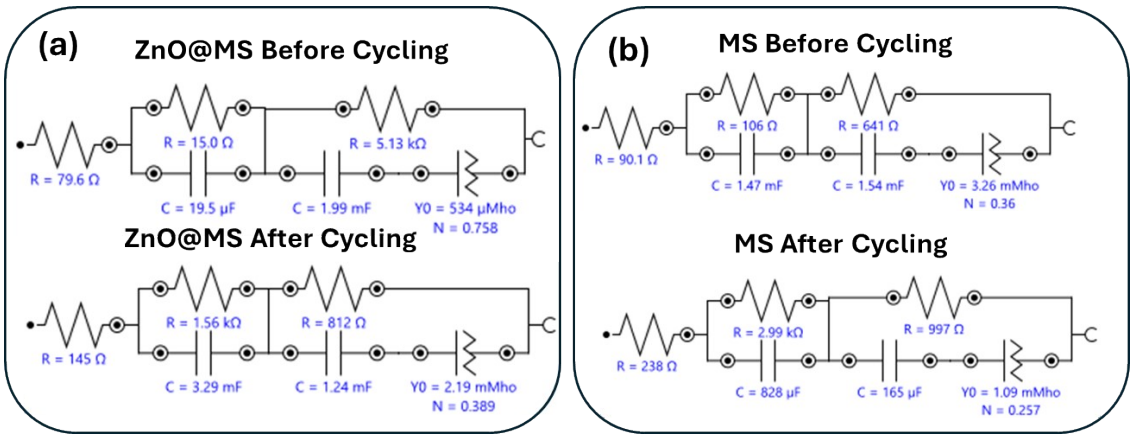

Figure S3: Fitted equivalent circuit for (a) ZnO@MS before cycling and after cycling, (b) MS before cycling and after cycling

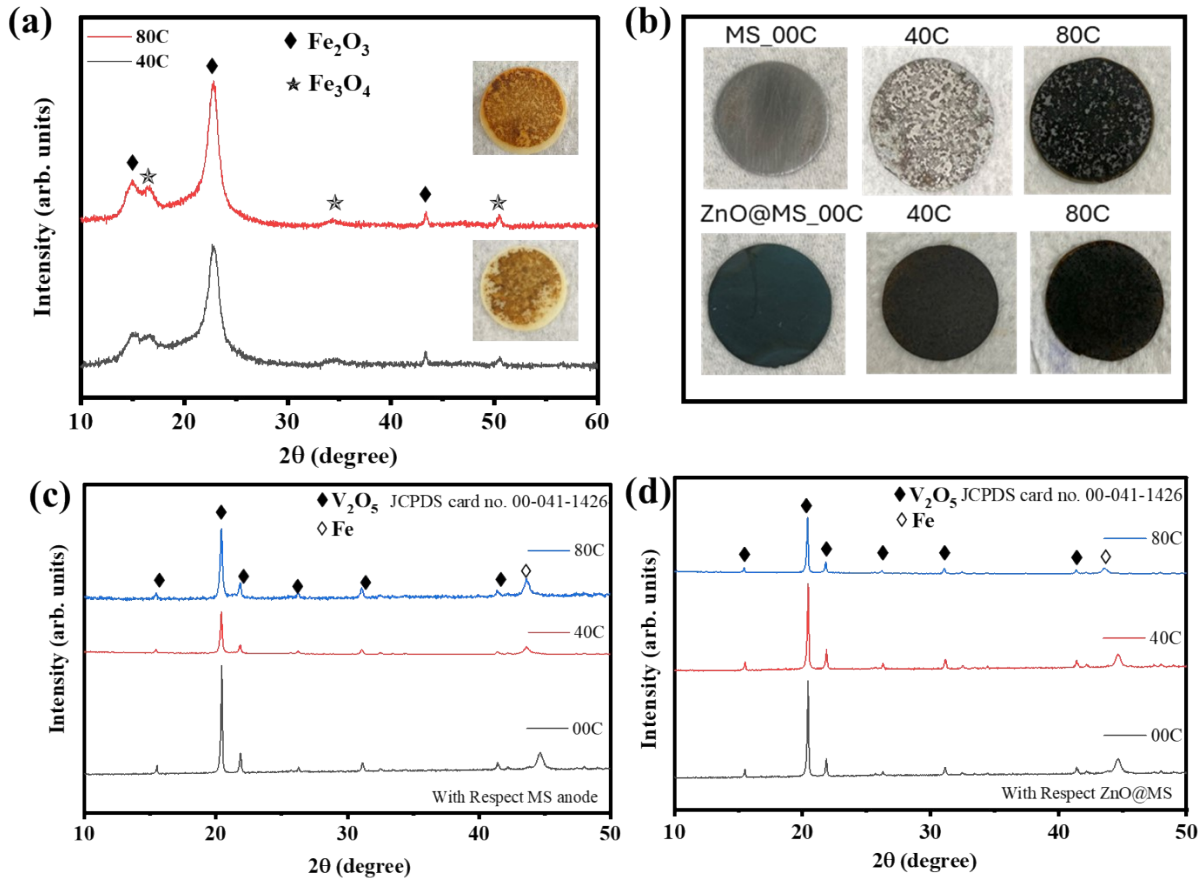

Figure S4: XRD Patterns (a) the of the separator sticked with anode residue after 40C and 80C in the presence of MS anode (b) Camera photograph of the MS and ZnO@MS for the different cycling, cathode (V_2O_5 coated SS) before cycling and after cycling of 40C and 80C (c) with respect to the MS and (d) ZnO@MS respective coin cells

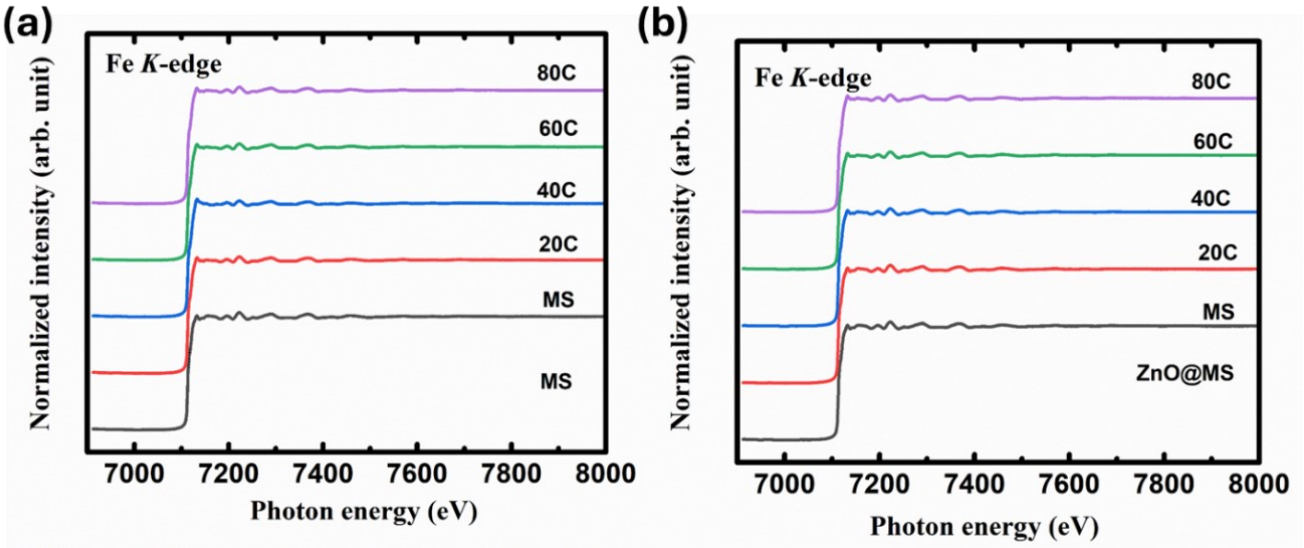

Figure S5: Fe *K*-edge EXAFS spectra of (a) MS and (b) ZnO@MS at different cycles

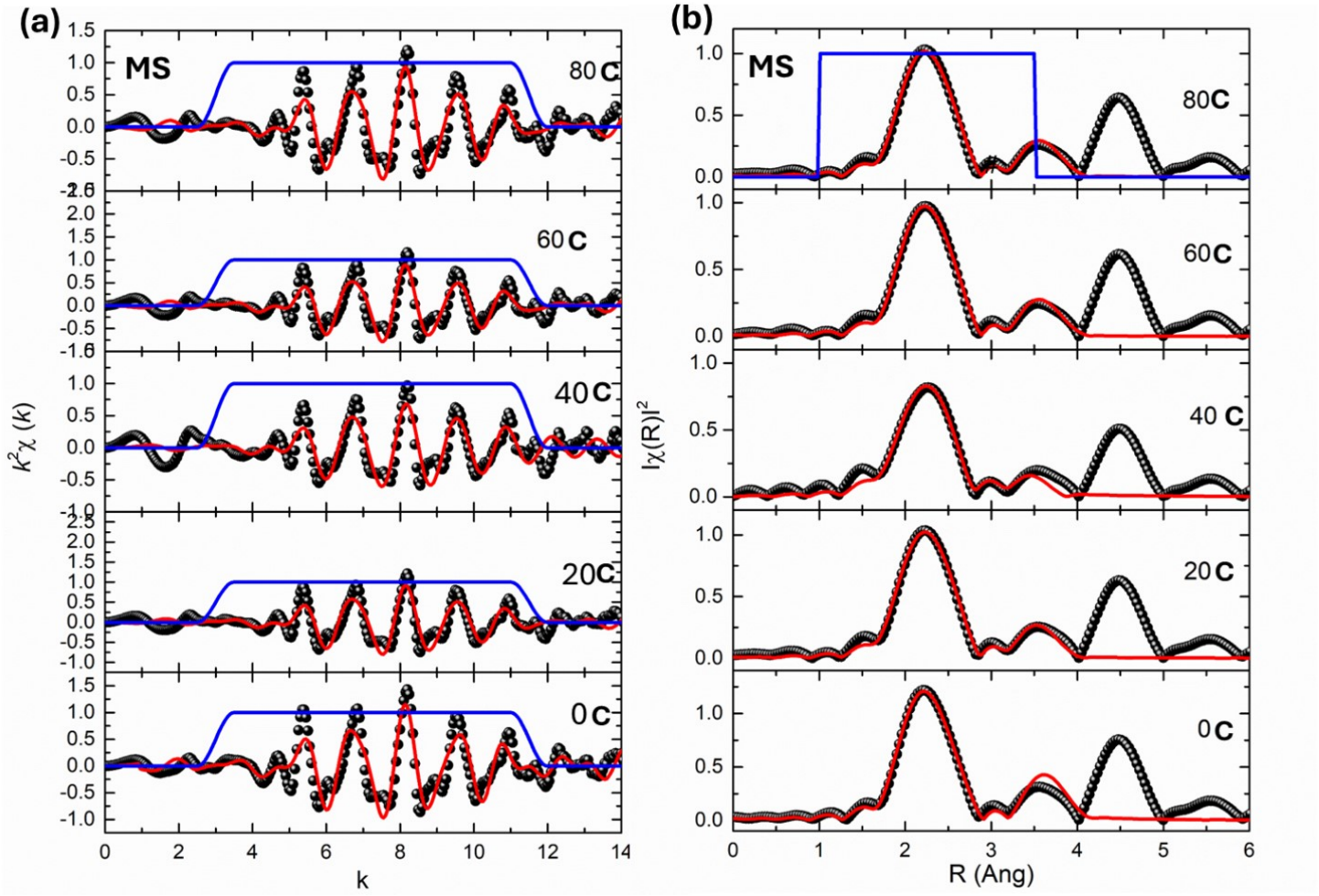

Figure S6: MS-based anode at different cycles (a) Simulated k^2-weight EXAFS spectra for (b) Simulated non-phase corrected Fourier Transform of EXAFS spectra

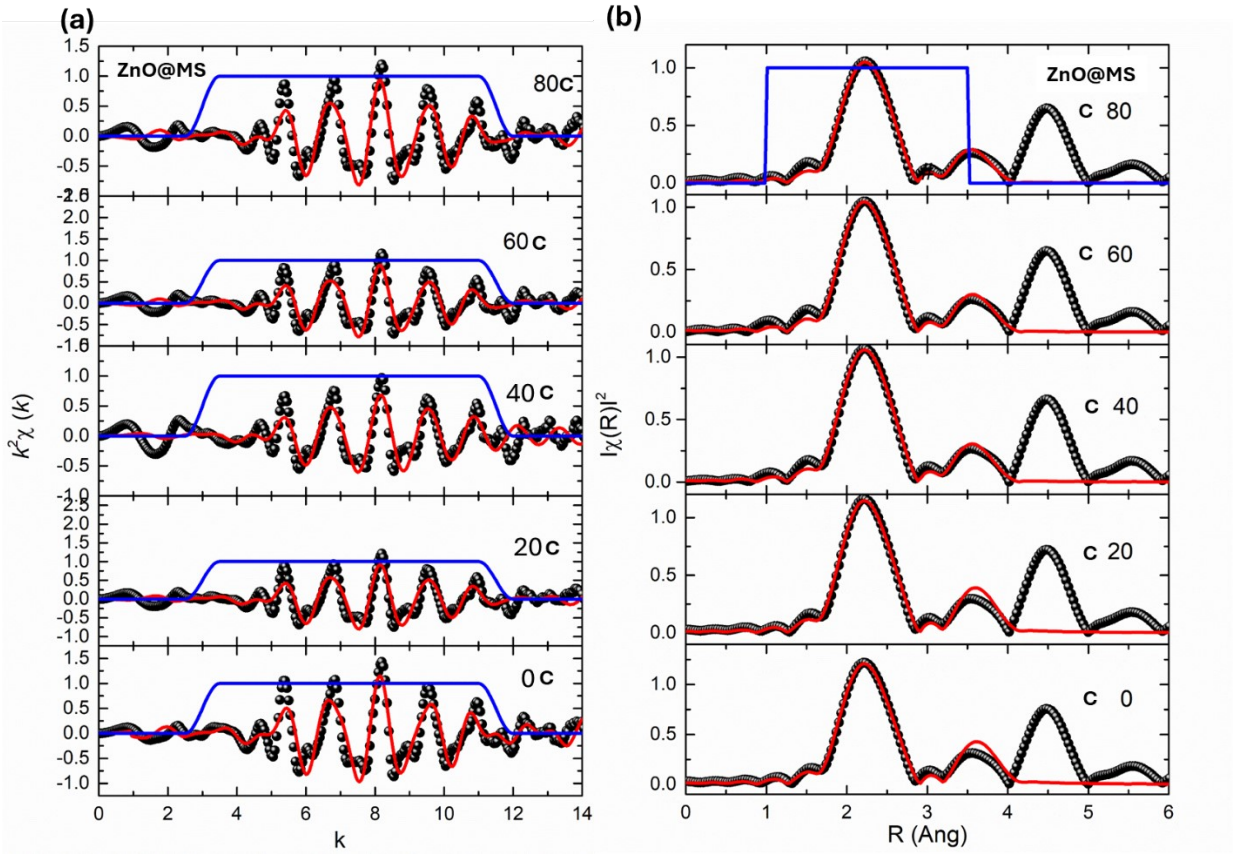

Figure S7: ZnO@MS based anode at different cycles (a) simulated k^2-weight EXAFS spectra (b) Simulated non-phase corrected Fourier Transform of EXAFS spectra

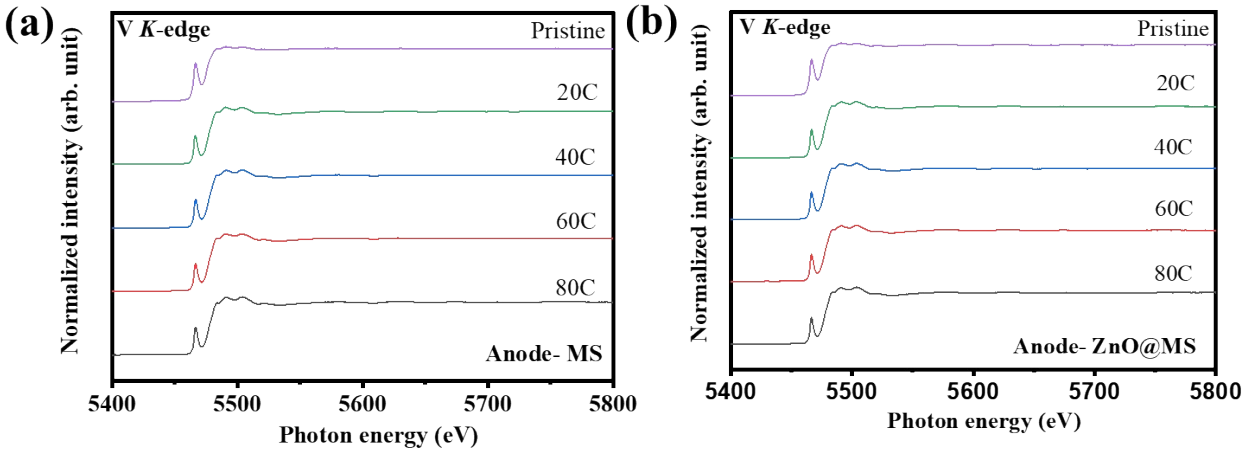

Figure S8: V *K*-edge EXAFS spectra of V_2O_5 cathodes with (a) MS and (b) ZnO@MS anodes at different cycles

Table S1: Main edge Energy of MS and ZnO@MS anodes at various cycles

No of Cycles	Main Edge Energy (eV)- Half of Step

	Height	
	MS	**ZnO@MS**
0	7113.7	7113.7
20	7113.9	7113.7
40	7114.2	7113.8
60	7113.9	7113.8
80	7113.8	7114.0

Table S2: Coordination number (N), radial distance (R), Debye-Waller factor (σ^2) and correction to main energy (ε_o) at different cycle stages for pristine MS and ZnO@MS based anode material in Fe-ion batteries.

Stages	Shell	N	R (Å)	σ^2 (Å^2)	ε_o (eV)	R-factor
0	Fe-Fe	7.5±1.0	2.445±0.004	0.002±0.001	3.1	0.007
	Fe-Fe	6.2±0.5	2.833±0.007	0.002		
	Fe-Fe	11.6±2.7	3.998±0.016	0.003		
MS_20C	Fe-Fe	6.2±0.9	2.431±0.004	0.002±0.001	-1.7	0.007
	Fe-Fe	6.5±0.4	2.805±0.005	0.002		
	Fe-Fe	11.5±2.4	3.958±0.015	0.007		
ZnO@MS_20C	Fe-Fe	7.1±0.9	2.445±0.004	0.002±0.001	2.3	0.007
	Fe-Fe	6.2±0.5	2.829±0.006	0.002		
	Fe-Fe	11.2±2.6	3.991±0.015	0.003		
MS_40C	Fe-Fe	6.1±0.55	2.418±0.006	0.006±0.001	-8.0	0.02
	Fe-Fe	6.5±0.5	2.765±0.004	0.002		
	Fe-Fe	11.6±3.8	3.893±0.026	0.012		
ZnO@MS_40C	Fe-Fe	6.1±0.8	2.437±0.003	0.002±0.001	0.2	0.007
	Fe-Fe	6.1±0.4	2.818±0.005	0.002		
	Fe-Fe	11.8±2.5	3.976±0.015	0.006		
MS_60C	Fe-Fe	6.0±0.8	2.419±0.003	0.002±0.001	0.2	0.006
	Fe-Fe	6.0±0.4	2.804±0.005	0.002		
	Fe-Fe	11.6±2.4	3.982±0.015	0.007		
ZnO@MS_60C	Fe-Fe	5.9±0.9	2.438±0.003	0.002±0.001	0.6	0.007
	Fe-Fe	6.0±0.4	2.820±0.006	0.002		
	Fe-Fe	11.5±2.7	3.983±0.016	0.006		
MS_80C	Fe-Fe	6.0±0.8	2.421±0.003	0.002±0.001	0.1	0.005
	Fe-Fe	6.1±0.4	2.805±0.004	0.002		
	Fe-Fe	11.7±2.2	3.979±0.013	0.006		
ZnO@MS_80C	Fe-Fe	5.9±0.9	2.433±0.003	0.002±0.001	-0.6	0.007
	Fe-Fe	6.1±0.4	2.812±0.005	0.001		
	Fe-Fe	11.6±2.5	3.969±0.015	0.006		